https://ntrs.nasa.gov/search.jsp?R=19930086336 2020-06-17T12:39:39+00:00Z

NACA RM-L50H17a 30

RESTRICTED UNCLASSIFIED

Copy
RM L50H17a

Classification Changed to
UNCLASSIFIED
NACA Research Abstract #19
dated May 19, 1952
2/28/52
Date 6/23/52 By J. E. Newlan NCA

CASE FILE COPY

NACA

RESEARCH MEMORANDUM

A METHOD FOR PREDICTING THE LOW-SPEED CHORDWISE PRESSURE DISTRIBUTION OVER SHARP-EDGE AIRFOIL SECTIONS WITH PLAIN FLAPS AT THE LEADING AND TRAILING EDGES

By Robert J. Nuber and Jones F. Cahill

Langley Aeronautical Laboratory
Langley Air Force Base, Va.

JPL LIBRARY
CALIFORNIA INSTITUTE OF TECHNOLOGY

CLASSIFIED DOCUMENT

This document contains classified information affecting the National Defense of the United States within the meaning of the Espionage Act, USC 50:31 and 32. Its transmission or the revelation of its contents in any manner to an unauthorized person is prohibited by law.

Information so classified may be imparted only to persons in the military and naval services of the United States, appropriate civilian officers and employees of the Federal Government who have a legitimate interest therein, and to United States citizens of known loyalty and discretion who of necessity must be informed thereof.

NATIONAL ADVISORY COMMITTEE
FOR AERONAUTICS

WASHINGTON
October 2, 1950

RESTRICTED UNCLASSIFIED

OCT 10 1950

Classification Changed to
UNCLASSIFIED
Authority NACA Research Abstract #19, dated Mar. 19, 1952. 2/28/52
Date 6/23/52 By J.E. Neulan NCA

RESTRICTED
UNCLASSIFIED

NATIONAL ADVISORY COMMITTEE FOR AERONAUTICS

RESEARCH MEMORANDUM

A METHOD FOR PREDICTING THE LOW-SPEED CHORDWISE PRESSURE DISTRIBUTION OVER SHARP-EDGE AIRFOIL SECTIONS WITH PLAIN FLAPS AT THE LEADING AND TRAILING EDGES

By Robert J. Nuber and Jones F. Cahill

SUMMARY

A method is presented for the calculation of the low-speed chordwise pressure distribution over various sharp-edge airfoils equipped with leading-edge and trailing-edge flaps of arbitrary size and deflection. The method was developed from an analysis and correlation of experimental pressure-distribution data obtained from an investigation of a sharp-edge airfoil having leading-edge and trailing-edge flaps. The generalization of the data obtained from tests of a single airfoil to apply to other relatively thin sharp-edge airfoils rests on the fundamental assumption that for sharp-edge airfoils the separation phenomena controlling those components of the pressure distribution which can not be calculated from potential-flow theory do not vary appreciably with variations in the detailed shape of the airfoil.

INTRODUCTION

Thin sharp-edge wings designed to minimize wave resistance have been proposed for use on high-speed aircraft. As a result, leading-edge high-lift devices are required for satisfactory low-speed characteristics and the necessity has arisen of obtaining adequate section load data for such lift augmenters in conjunction with trailing-edge flaps. An investigation has accordingly been made in the Langley two-dimensional low-turbulence tunnel of the aerodynamic loads over leading-edge and trailing-edge plain flaps (0.15 chord and 0.20 chord, respectively) on a 6-percent-thick symmetrical circular-arc airfoil section (reference 1).

In an effort to provide the designer with additional section load information, a generalized method has been developed from an analysis of data of reference 1 which permits the determination of the chordwise

RESTRICTED
UNCLASSIFIED

pressure distribution over sharp-edge airfoils equipped with leading- and trailing-edge flaps of arbitrary size and deflection. The development of the method is presented in this paper together with an illustrative example.

COEFFICIENTS AND SYMBOLS

c_l airfoil-section lift coefficient $\left(\frac{l}{qc}\right)$

c_{l_i} airfoil-section ideal lift coefficient; lift coefficient at which stagnation point occurs at leading edge

$c_{l_{b\delta}}$ change in ideal lift coefficient caused by flap deflection

c_{l_a} airfoil-section additional lift coefficient due to angle of attack $\left(c_l - c_{l_{b\delta}}\right)$

S surface pressure coefficient $\left(\frac{H_o - p}{q}\right) = \left(\frac{v}{V}\right)^2$ (in incompressible flow)

P pressure-difference coefficient across airfoil $\left(\frac{p_U - p_L}{q}\right)$

c_n flap-section normal-force coefficient $\left(\frac{n}{qc_f}\right)$

c_h flap-section hinge-moment coefficient $\left(\frac{h}{qc_f^2}\right)$

l airfoil lift per unit span

H_o free-stream total pressure

p local static pressure

n flap normal force per unit span, positive upward

h flap hinge moment per unit span, positive when trailing edge tends to deflect downward or leading edge upward

c airfoil chord

c_f flap chord

q	free-stream dynamic pressure $\left(\frac{\rho V^2}{2}\right)$
ρ	free-stream density
V	free-stream velocity
α_o	airfoil-section angle of attack, degrees
δ	flap deflection, positive when deflected below chord line, degrees
v	local velocity on airfoil surface
v'	incremental local velocity on airfoil surface due to separation
Δv_a	additional local velocity on airfoil surface due to departure from the ideal lift coefficient
x	distance behind leading edge, inches
E	$\left(\frac{c_f}{c}\right)$
R	Reynolds number $\left(\frac{Vc}{\nu}\right)$
ν	kinematic viscosity

Subscripts:

N	leading-edge flap
F	trailing-edge flap
i	ideal
U	upper surface
L	lower surface
$b\delta$	refers to conditions at the ideal lift coefficient with flap deflected
a	refers to difference between conditions at the ideal lift coefficient and any arbitrary lift coefficient

DERIVATION OF METHOD

Velocity distributions as calculated by potential-flow methods generally bear little resemblance to those obtained experimentally on sharp-edge airfoils because of the existence of extensive regions of separated flow. When analysing the velocity distribution about sharp-edge airfoils with flaps, however, it is convenient for the resultant distribution to be broken down into various component parts as is done in the case of airfoils in potential flow (reference 2). The most generally used breakdown considers the resultant velocity distribution to be made up of the following three components:

(1) Distribution of velocity about the basic symmetrical airfoil at zero angle of attack v/V

(2) Incremental additional velocity distribution due to departure of the airfoil from the ideal lift coefficient $\Delta v_a/V$

(3) Mean-line velocity distribution

(a) Caused by airfoil camber $\Delta v/V$

(b) Caused by flap deflection $(\Delta v/V)_{b\delta}$

In the present paper, the only type of mean-line velocity distribution considered is that resulting from flap deflection, since the data used in the analysis are for a symmetrical airfoil section.

In terms of the three-component velocities, the complete velocity distribution about an airfoil at any lift coefficient is given approximately by:

$$\sqrt{S_U} = \frac{v}{V} + \frac{\Delta v_a}{V} + \left(\frac{\Delta v}{V}\right)_{b\delta} \tag{1}$$

$$\sqrt{S_L} = \frac{v}{V} - \frac{\Delta v_a}{V} - \left(\frac{\Delta v}{V}\right)_{b\delta} \tag{2}$$

For the basic thickness form at zero lift, the velocity distribution can, in any case, be calculated by the methods of references 3 and 4. In the absence of flow separation, the component $\Delta v_a/V$ is usually taken

to be a linear function of the additional lift coefficient c_{l_a}, that is, the difference between any arbitrary lift coefficient and the ideal lift coefficient, and can be calculated by thick-airfoil theory. If extensive regions of separation do not exist, the component $\Delta v/V$ resulting from airfoil camber or flap deflection can also be calculated. The methods of thin-airfoil theory (references 5 and 6) are usually employed for this purpose.

For sharp-edge airfoils on which flow separation limits the applicability of potential-flow methods, the problem of developing a general method of determining the velocity distribution resolves itself into a determination of the manner in which the various component distributions vary with c_{l_a} and δ. First, the manner in which the additional velocity distribution $\Delta v_a/V$ varies with the additional lift coefficient must be found. The use of the experimental pressure-distribution data of reference 1 and the following relation provides the solution:

$$\frac{\Delta v_a}{V} = \frac{\sqrt{S_U} - \sqrt{S_L}}{2} - \left(\frac{\Delta v}{V}\right)_{b\delta} \tag{3}$$

Next, the extent to which the theoretical velocity distribution due to flap deflection is realized experimentally must be determined. In order to determine the variation of $\Delta v_a/V$ with lift coefficient and the comparison of the experimental and theoretical velocity distributions, the ideal lift coefficient must be known. For any combination of leading-edge and trailing-edge flap deflections, the ideal lift coefficient can be calculated by the methods of reference 5; however, because of flow separation, a correlation must be made between the theoretical and experimental ideal lift coefficients. Finally, it becomes necessary to determine the velocity distribution about the basic thickness form at zero lift, that is, by definition:

$$\frac{v}{V} = \frac{\sqrt{S_U} + \sqrt{S_L}}{2} \tag{4}$$

The value of v/V for the symmetrical airfoil at zero lift can, of course, be calculated by potential-flow methods; however, the extent of the separated flow on the upper and lower surfaces and, therefore, the effective value of v/V which must be used in equations (1) and (2) vary with lift coefficient and flap deflection. Consequently, the value of v/V for the symmetrical airfoil at zero lift, determined theoretically, must be corrected by an increment v'/V which is a function of

lift coefficient and flap deflection. The value of v'/V will be determined from the data of reference 1.

Although the method to be presented is developed on the basis of data from tests of only one airfoil section, it is thought that the results may be generally applied to other relatively thin sharp-edge airfoil sections because, for such airfoils, the separation phenomena controlling those components of the pressure distribution which cannot be calculated from potential-flow theory, would not be expected to vary appreciably with variations in the shape of the airfoil.

Ideal lift coefficient.- As indicated previously, a knowledge of the association between the theoretical and experimental ideal lift coefficients resulting from flap deflection, $c_{l_{b\delta}}$, is essential. The change in ideal lift coefficient is equal to the sum of two-component changes, one resulting from leading-edge-flap deflection and the other from trailing-edge-flap deflection. Each of these components may be calculated separately and added linearly. For each leading-edge- and trailing-edge-flap deflection investigated in reference 1, the lift coefficient at which the stagnation point occurred at the leading edge, $c_{l_{b\delta}}$, has been determined from the experimental data. The results are compared in figure 1 with those calculated from thin-airfoil theory. As shown in figure 1 the experimental values of $c_{l_{b\delta}}$ vary almost linearly with trailing-edge-flap deflection above 10° and, for the leading-edge flap, the theoretical coefficients are identical with those obtained experimentally. In calculating the ideal lift coefficients $c_{l_{b\delta_N}}$ resulting from deflection of a leading-edge flap, the theoretical value may, therefore, be used.

For trailing-edge-flap deflections above 10°, the experimentally determined values of the ideal lift coefficient $c_{l_{b\delta_F}}$ are considerably lower than indicated by the theory. In order to provide a means of determining the change in ideal lift coefficient associated with deflection of trailing-edge flaps of different chords, Allen's equation, presented in reference 7, was used. In this equation the ideal normal-force coefficient is expressed as a function of flap-chord ratio, flap deflection, and pitching-moment increment resulting from flap deflection. Values of $c_{l_{b\delta_F}}$ (the normal-force coefficient was taken to be essentially the same as the lift coefficient) obtained by this method are plotted in figure 2 against trailing-edge-flap deflection for flap-chord ratios ranging between 10 and 50 percent. The values of the quarter-chord pitching-moment increment required for the determination of these curves were determined from numerous experimental data. These ideal lift coefficients (fig. 2) represent average values obtained from a series of tests of plain flaps on a large number of conventional airfoil

sections. Similar computations were also made for the 20-percent-chord flap on the circular-arc airfoil used in the present analysis and, as expected, the results were identical with the corresponding data in figure 2. For any profile with plain flaps, therefore, the results of figure 2 can be used for the determination of the ideal lift coefficient.

Mean-line velocity distribution.- The distribution of velocity resulting from flap deflection $(\Delta v/V)_{b\delta}$ was computed from the data of reference 1 for various flap deflections by means of the following equation:

$$\left(\frac{\Delta v}{V}\right)_{b\delta} = \frac{\left(\frac{v}{V}\right)_{i_U} - \left(\frac{v}{V}\right)_{i_L}}{2}$$

This expression was obtained by subtracting equation (2) from equation (1) since, by definition, $\Delta v_a/V$ is zero at the ideal lift coefficient. The data thus obtained for various deflections of the leading-edge flap were found to be very nearly independent of flap deflection when expressed in the form of $\left(\frac{\Delta v}{V}\right)_{b\delta_N} \Big/ c_{l_{b\delta_N}}$. A comparison of the mean value of $\left(\frac{\Delta v}{V}\right)_{b\delta_N} \Big/ c_{l_{b\delta_N}}$ plotted against percent chord as determined by theory and experiment (fig. 3(a)) shows good agreement. It is concluded, therefore, that the mean-line velocity distribution resulting from deflection of leading-edge flaps of various chords can be calculated theoretically with a sufficiently high degree of accuracy. Due to the effects of separation near the trailing edge, however, the experimental velocity distributions resulting from deflection of the plain trailing-edge flap differed markedly from those predicted by the theory, particularly for large flap deflections. A different distribution for each trailing-edge-flap deflection (reference 1) was determined, therefore, and the results are presented in figure 3(b) in the form of $(\Delta v/V)_{b\delta_F}$ against percent chord.

As a basis for extending the analysis to apply to sharp-edge airfoils having trailing-edge flap-chord ratios other than 0.20, the normal-force distribution $P_{b\delta_F}/c_{l_{b\delta_F}}$ was determined from the pressure distribution at the ideal lift coefficient for several trailing-edge-flap deflections by the following relation

$$\frac{P_{b\delta_F}}{c_{l_{b\delta_F}}} = \frac{\left(\frac{v}{V}\right)_{i_U}^2 - \left(\frac{v}{V}\right)_{i_L}^2}{c_{l_{b\delta_F}}} = \frac{4\left(\frac{\Delta v}{V}\right)_{b\delta}\left(\frac{v}{V}\right)}{c_{l_{b\delta_F}}}$$

When compared with the distributions presented in reference 7 for a 0.20c trailing-edge flap, good agreement was obtained. It is probable, therefore, that the normal-force distribution $P_{b\delta_F}/c_{l_{b\delta_F}}$, and consequently the velocity distribution, may be determined with satisfactory precision for any desired trailing-edge flap-chord ratio and deflection from table III of reference 7.

Additional velocity distribution.- The values of the local incremental velocity ratio $\Delta v_a/V$ were determined from the data of reference 1 and equation (3) and, when plotted as a function of the additional lift coefficient $\left(c_{l_a} = c_l - c_{l_{b\delta}}\right)$, were found to be essentially independent of either leading-edge- or trailing-edge-flap deflection. Average values of $\Delta v_a/V$ are plotted against c_{l_a} in figure 4 for various chordwise positions. It is thought that these values of $\Delta v_a/V$ (fig. 4) can be used for various flap-chord ratios since, after the leading edge has caused separation of the flow, any differences in airfoil contour behind that point would have only secondary effects on $\Delta v_a/V$.

Effective basic velocity distribution.- The velocity distribution v/V about the basic symmetrical airfoil (reference 1) at zero lift is presented in figure 5. As previously indicated, such velocity distributions can be calculated by the available theoretical methods given in references 3 and 4. The effective values of v/V which must be employed in equations (1) and (2), however, vary with both additional lift coefficient and trailing-edge-flap deflection because of separation phenomena. The increment v'/V which must be added to the theoretical basic velocity distribution was determined from the following relation:

$$\frac{v'}{V} = \frac{\left(\frac{v}{V}\right)_U + \left(\frac{v}{V}\right)_L}{2} - \frac{v}{V} \qquad (5)$$

Since v'/V is a function of both trailing-edge-flap deflection and lift coefficient, it may be broken down into two components; namely, $(v'/V)_F$ and $(v'/V)_a$, respectively. The values of $(v'/V)_F$ were determined first from equation (5) by using the experimental pressure distributions at the design lift coefficient. Values of the total change in basic velocity distribution $\left(\frac{v'}{V}\right) = \left(\frac{v'}{V}\right)_F + \left(\frac{v'}{V}\right)_a$ were determined

from equation (5) by using the experimental pressure distributions at various lift coefficients. From the results thus obtained, the values of $(v'/V)_F$ were subtracted to obtain $(v'/V)_a$. It should be pointed out that deflection of the nose flap had no appreciable effect on the shape of these velocity distributions when expressed as a function of c_{l_a}.

For various chordwise positions, values of $(v'/V)_F$ are presented in figure 6 as a function of trailing-edge-flap deflection. Forward of the 40-percent-chord station values of this component of velocity were found to be negligibly small. The chordwise position of $(v'/V)_F$ is expressed in terms of $\frac{x/c}{1 - E_F}$ and $\frac{1 - \frac{x}{c}}{E_F}$ for points ahead of and behind the hinge, respectively. In this form, the results are correlated so that they may be applied to sharp-edge airfoils having trailing-edge flaps of varying chord. This method of correlation is thought to be justified since the distribution of $(v'/V)_F$ is a result of separation at the flap hinge and has been shown (reference 7) to be similar for various hinge locations.

The results of the determinations of $(v'/V)_a$ are shown in figure 7. As would be expected, the values are independent of flap deflection when expressed in terms of c_{l_a}.

APPLICATION OF METHOD

In order to demonstrate the application of the method derived above, the computations required to determine the pressure coefficient at 55 percent of the chord of a 6-percent-thick symmetrical circular-arc airfoil section with a 10-percent-chord leading-edge flap deflected 30° and a 30-percent-chord trailing-edge flap deflected 40° are worked out in the following example. The section lift coefficient is assumed to be 1.65.

Lift-coefficient increments:

From reference 7,

$$c_{l_{b\delta_N}} = 2 \sin \theta_o \delta_N = 0.628$$

From figure 2,

$$c_{l_{b\delta_F}} = 0.772$$

Therefore,

$$c_{l_a} = 1.65 - (0.628 + 0.772) = 0.25$$

Airfoil basic velocity:

From figure 5 (or from theoretical calculations)

$$\frac{v}{V} = 1.078$$

Incremental additional velocity:

From figure 4 for $c_{l_a} = 0.250$,

$$\frac{\Delta v_a}{V} = 0.034$$

Mean-line velocity:

The local incremental basic velocities are computed from reference 7 in terms of the pressure-difference coefficient $P_{b\delta}$

From the theoretical relation (equation A-19, reference 7),

$$P_{b\delta_N} = 0.416$$

From table III (d) of reference 7,

$$P_{b\delta_F} = 1.639$$

Incremental velocity due to separation:

For $x/c = 0.55$,

$$\frac{x/c}{1 - E} = 0.786$$

And from figure 6,

$$\left(\frac{v'}{V}\right)_F = -0.062$$

From figure 7

$$\left(\frac{v'}{V}\right)_\alpha = -0.006$$

Pressure coefficient:

Rewriting equation 6 of reference 8,

$$S = \left(\frac{v}{V} \pm \frac{P_{b\delta}}{4 \frac{v}{V}} \right)^2$$

where v/V is the total of all the other v/V terms $\left(\text{excepting } (\Delta v/V)_{b\delta}\right)$

and $P_{b\delta}$ is the total of $P_{b\delta_N}$ and $P_{b\delta_F}$,

$$S_U = 2.361$$

$$S_L = 0.202$$

ACCURACY AND LIMITATIONS OF METHOD

In order to justify the method of correlation employed in the development of the present method, the calculated pressure distributions over the 6-percent-thick symmetrical circular-arc airfoil section and the integrated flap normal-force and hinge-moment coefficients for several individual and combined deflections of the plain leading-edge and trailing-edge flaps are compared with those obtained experimentally (reference 1) in figures 8 to 10. The flap pressure coefficients (fig. 8) are plotted against the projected chordwise position of the flap orifices on the airfoil chord. The dispersion of the normal-force and hinge-moment results shown in figures 9 and 10 may be considered typical of the accuracy to be expected from the present method. For individual deflections of the leading-edge and trailing-edge flaps the normal force and hinge-moment characteristics, as a rule, are within 10 percent of the experimental values. For combined deflections of the leading-edge and trailing-edge flaps, the predicted values of the loads and hinge moments over the trailing-edge flap remain within 10 percent; whereas, for the leading-edge flap the method tends to underestimate these characteristics to a larger degree, depending upon the magnitude of the flap deflections.

The flap hinges were located on the lower surface of the airfoil and the flaps were in contact with the flap skirts so that, in effect, there was no leakage of air between the upper and lower surfaces. It is believed that changes in the vertical location of the hinge line will have negligible effects on the airfoil characteristics. If leakage at

the flap hinge were present, however, the effects may be such as to alter the separation phenomena particularly at low trailing-edge-flap deflections.

Although there may be some tendency of increased Reynolds number to alter the conditions of the boundary layer, the effects of scale will probably be of an insignificant nature particularly in view of the negligible variations in section lift coefficient associated with sharp-edge airfoils. (See references 9, 10, and 11.)

CONCLUDING REMARKS

The experimental pressure distributions obtained for a 6-percent-thick circular-arc airfoil with various deflections of a leading- and trailing-edge flap have been analysed. The components of the pressure distribution attributable to the basic thickness form, change in angle of attack, and flap deflection have been expressed in such a form that they may be applied to the calculation of the pressure distribution about various sharp-edge airfoils having different flap sizes and deflections. The application of these results to other relatively thin sharp-edge airfoils rests on the fundamental assumption that, for such airfoils, the separation phenomena which control those portions of the pressure distribution that cannot be calculated by potential-flow theory do not vary appreciably with variations in the detailed shape of the airfoil. This assumption seems to be justified in large measure by the fact that the numerous pressure distributions obtained for the 6-percent-thick airfoil having various combinations of leading- and trailing-edge-flap deflections could be analyzed and correlated in terms which do not explicitly involve the flap deflection. Comparison of pressure distributions and integrated force coefficients obtained by the generalized method presented with some of the experimental data employed in the development of the method indicates that the methods by which the data were generalized give over-all results which are in reasonable agreement with experiment.

Langley Aeronautical Laboratory
National Advisory Committee for Aeronautics
Langley Air Force Base, Va.

REFERENCES

1. Underwood, William J., and Nuber, Robert J.: Aerodynamic Load Measurements over Leading-Edge and Trailing-Edge Plain Flaps on a 6-Percent-Thick Symmetrical Circular-Arc Airfoil Section. NACA RM L7H04, 1947.

2. Abbott, Ira H., Von Doenhoff, Albert E., and Stivers, Louis S., Jr.: Summary of Airfoil Data. NACA Rep. 824, 1945.

3. Theodorsen, T., and Garrick, I. E.: General Potential Theory of Arbitrary Wing Sections. NACA Rep. 452, 1933.

4. Theodorsen, Theodore, and Naiman, Irven: Pressure Distributions for Representative Airfoils and Related Profiles. NACA TN 1016, 1946.

5. Glauert, H.: Theoretical Relationships for an Aerofoil with Hinged Flap. R. & M. No. 1095, British A.R.C., 1927.

6. Glauert, H.: A Theory of Thin Aerofoils. R. & M. No. 910, British A.R.C., 1924.

7. Allen, H. Julian: Calculation of the Chordwise Load Distribution over Airfoil Sections with Plain, Split, or Serially Hinged Trailing-Edge Flaps. NACA Rep. 634, 1938.

8. Allen, H. Julian: A Simplified Method for the Calculation of Airfoil Pressure Distribution. NACA TN 708, 1939.

9. Underwood, William J., and Nuber, Robert J.: Two-Dimensional Wind-Tunnel Investigation at High Reynolds Numbers of Two Symmetrical Circular-Arc Airfoil Sections with High-Lift Devices. NACA RM L6K22, 1947.

10. Nuber, Robert J., and Cheesman, Gail A.: Two-Dimensional Wind-Tunnel Investigation of a 6-Percent-Thick Symmetrical Circular-Arc Airfoil Section with Leading-Edge and Trailing-Edge High-Lift Devices Deflected in Combination. NACA RM L9G20, 1949.

11. Powter, G. J., and Young, A. D.: Wind Tunnel Tests on a 7.5-Per Cent Thick Bi-Convex Wing with Leading and Trailing Edge Flaps. Rep. No. Aero. 2157, British R.A.E., Sept. 1946.

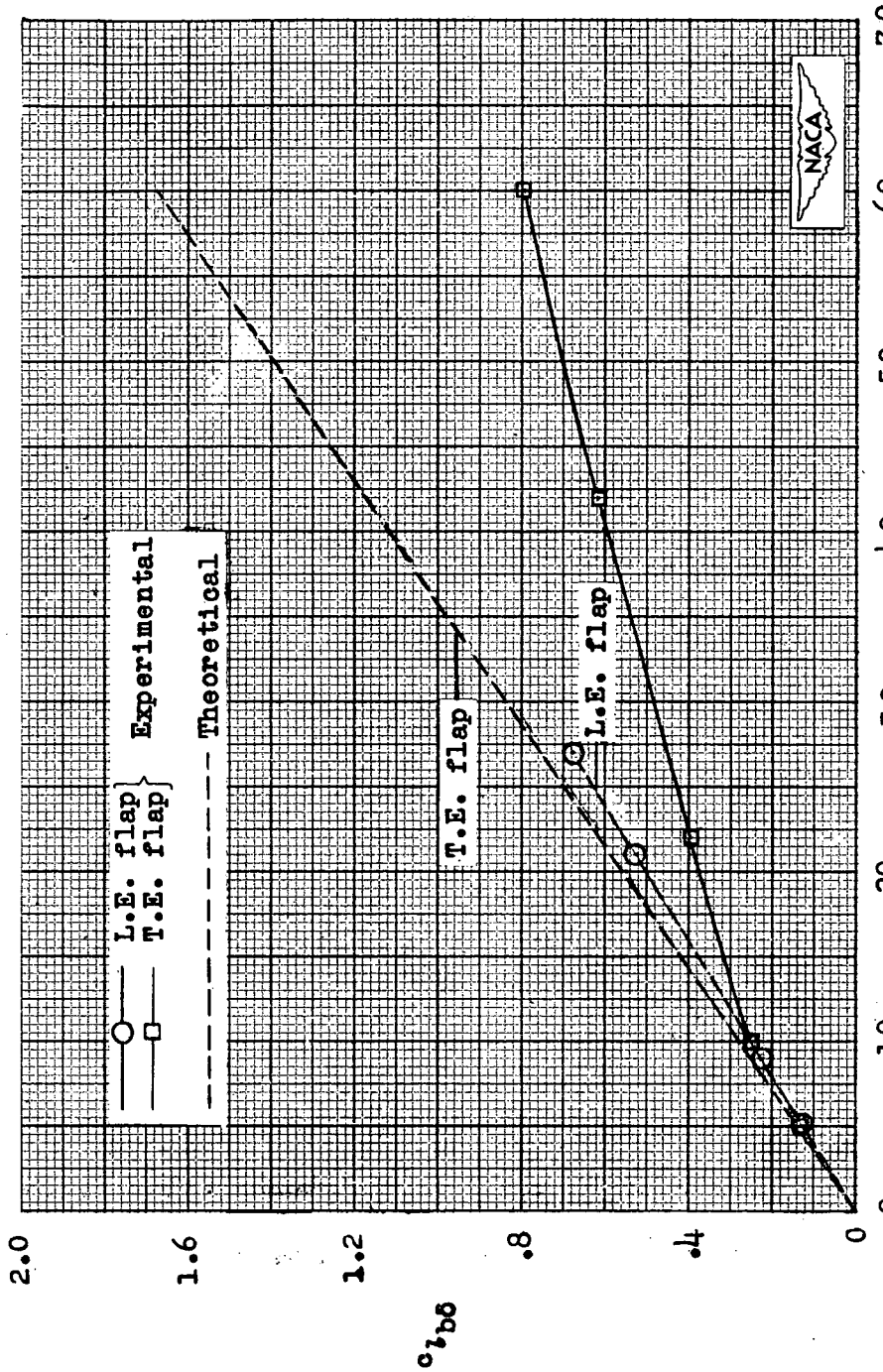

Figure 1.- Variation of change in ideal lift coefficient with deflection of the 0.15c plain leading-edge flap and 0.20c plain trailing-edge flap on the 6-percent-thick symmetrical circular-arc airfoil section (reference 1).

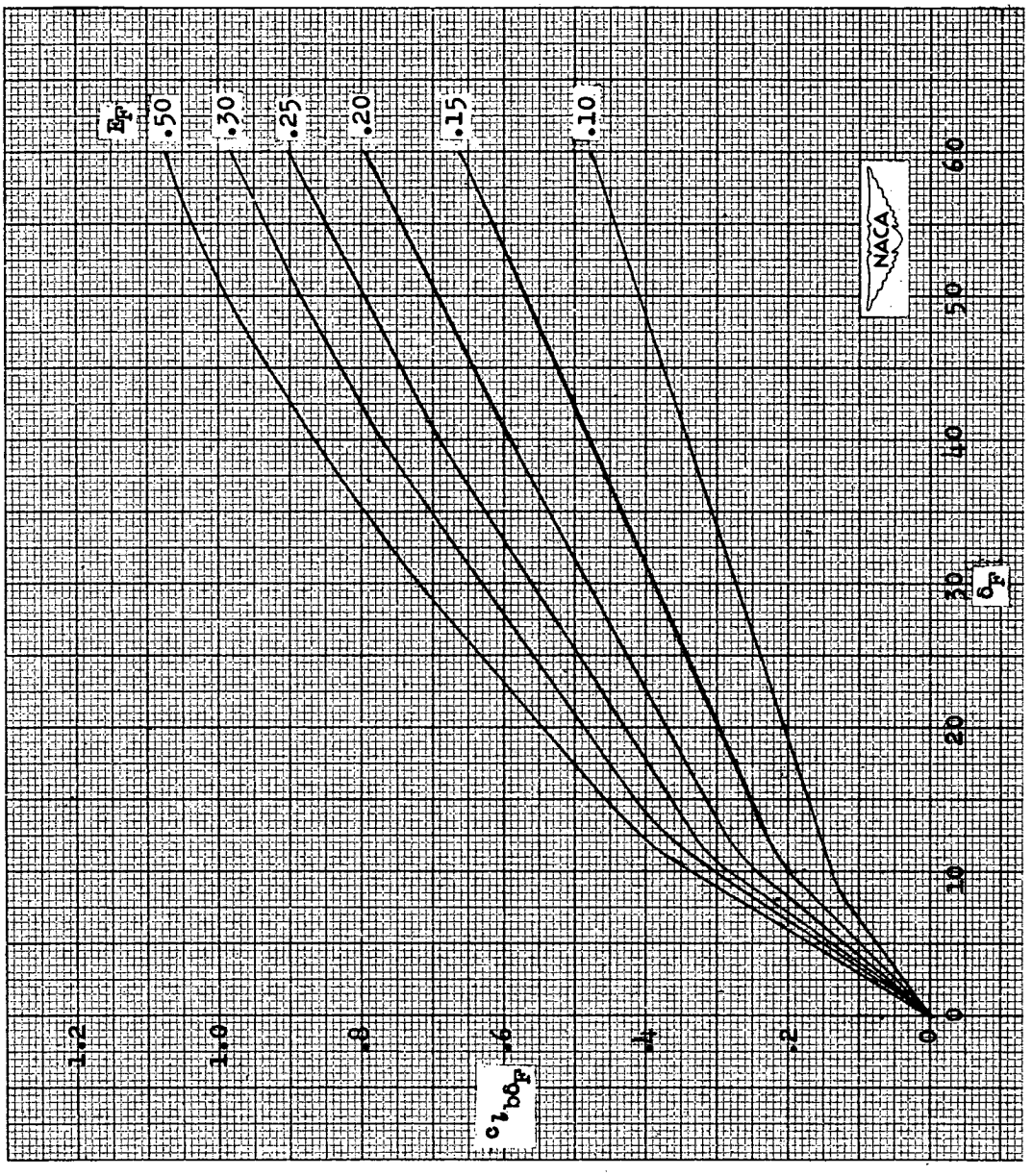

Figure 2.- Variation of change in ideal lift coefficient with plain trailing-edge-flap deflection.

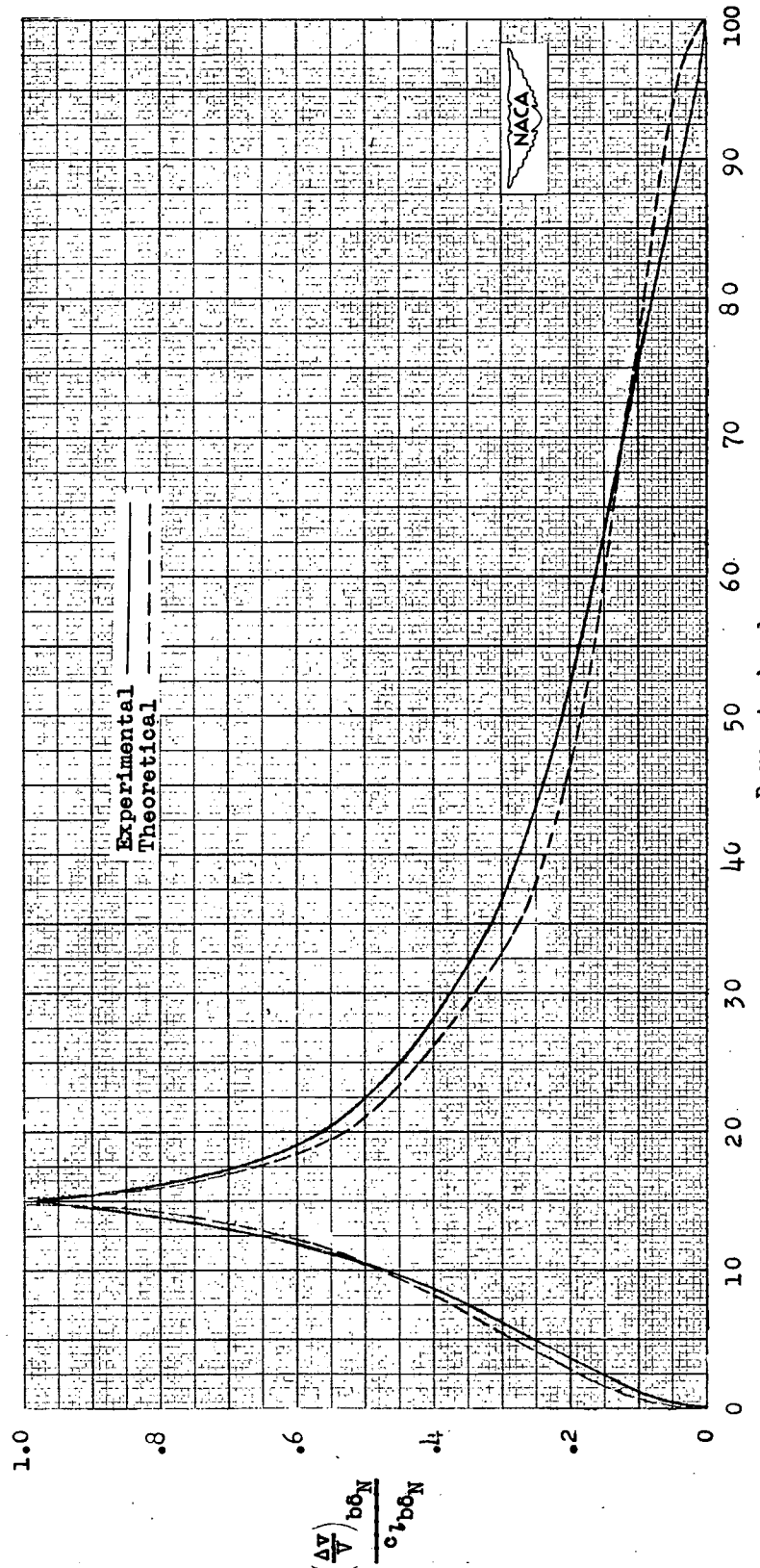

(a) 0.15c plain leading-edge flap.

Figure 3.- Mean line velocity distribution for various flap deflections.

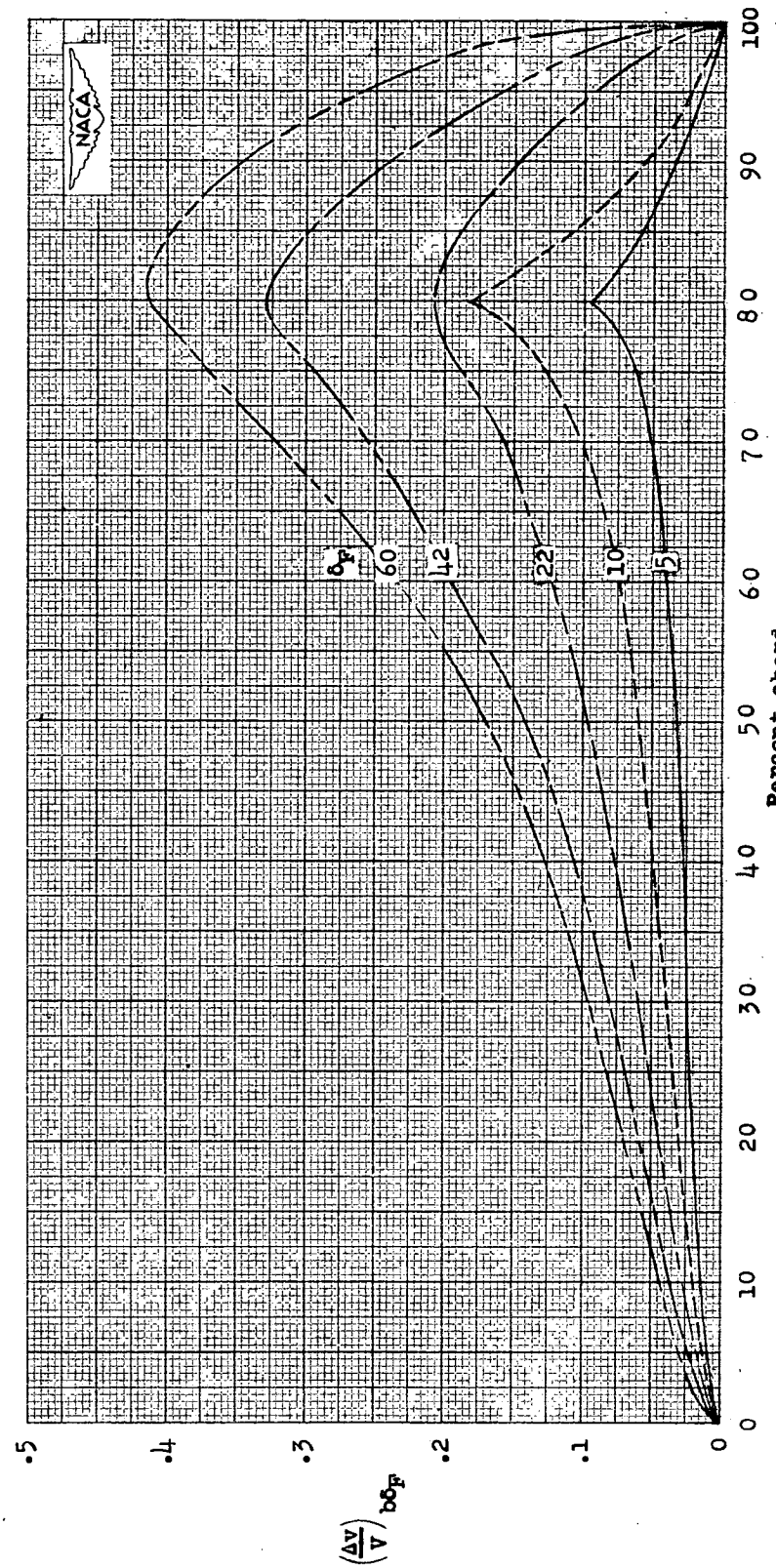

(b) 0.20c plain trailing-edge flap.

Figure 3.- Concluded.

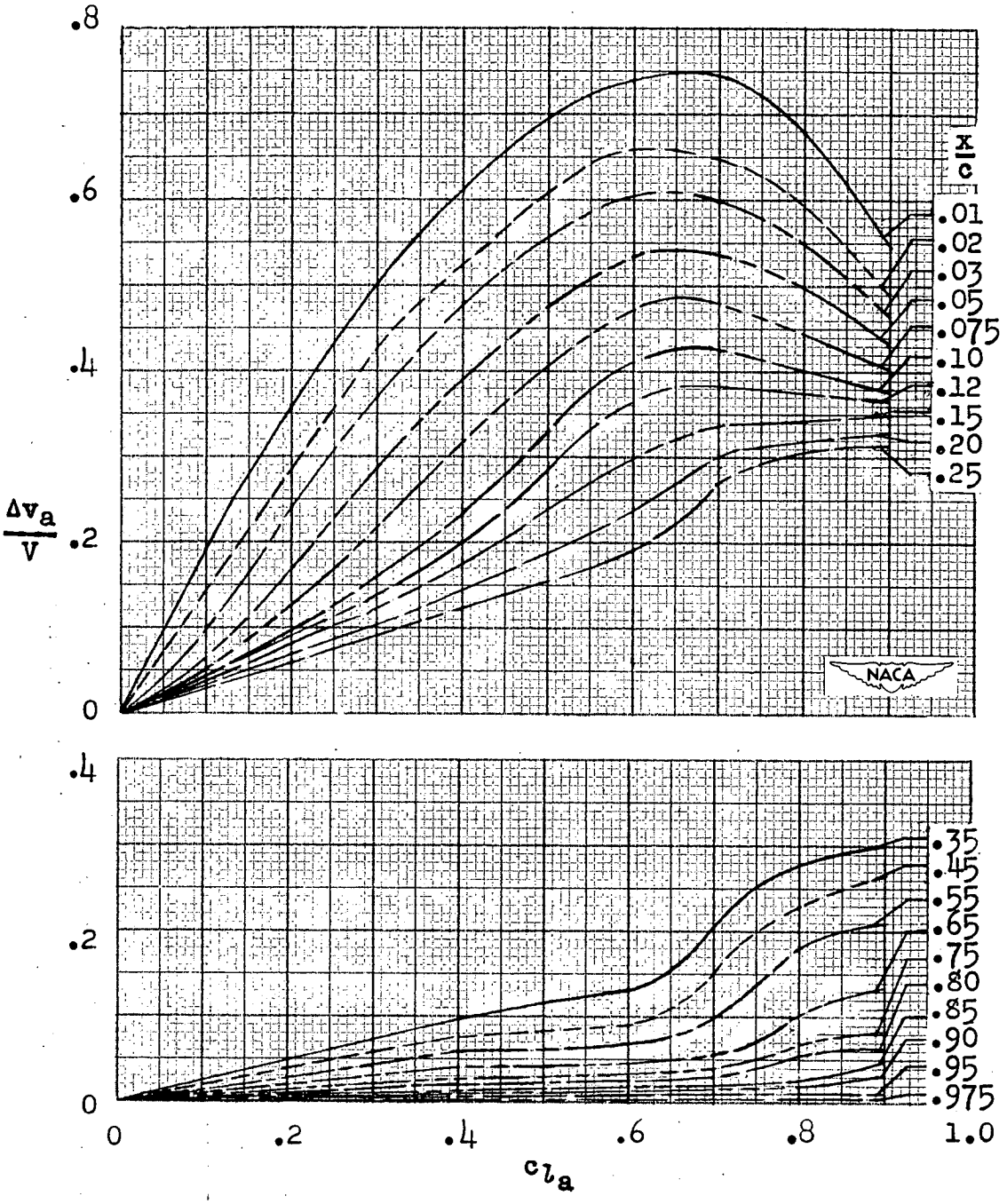

Figure 4.- Variation of incremental additional velocity ratio with additional lift coefficient.

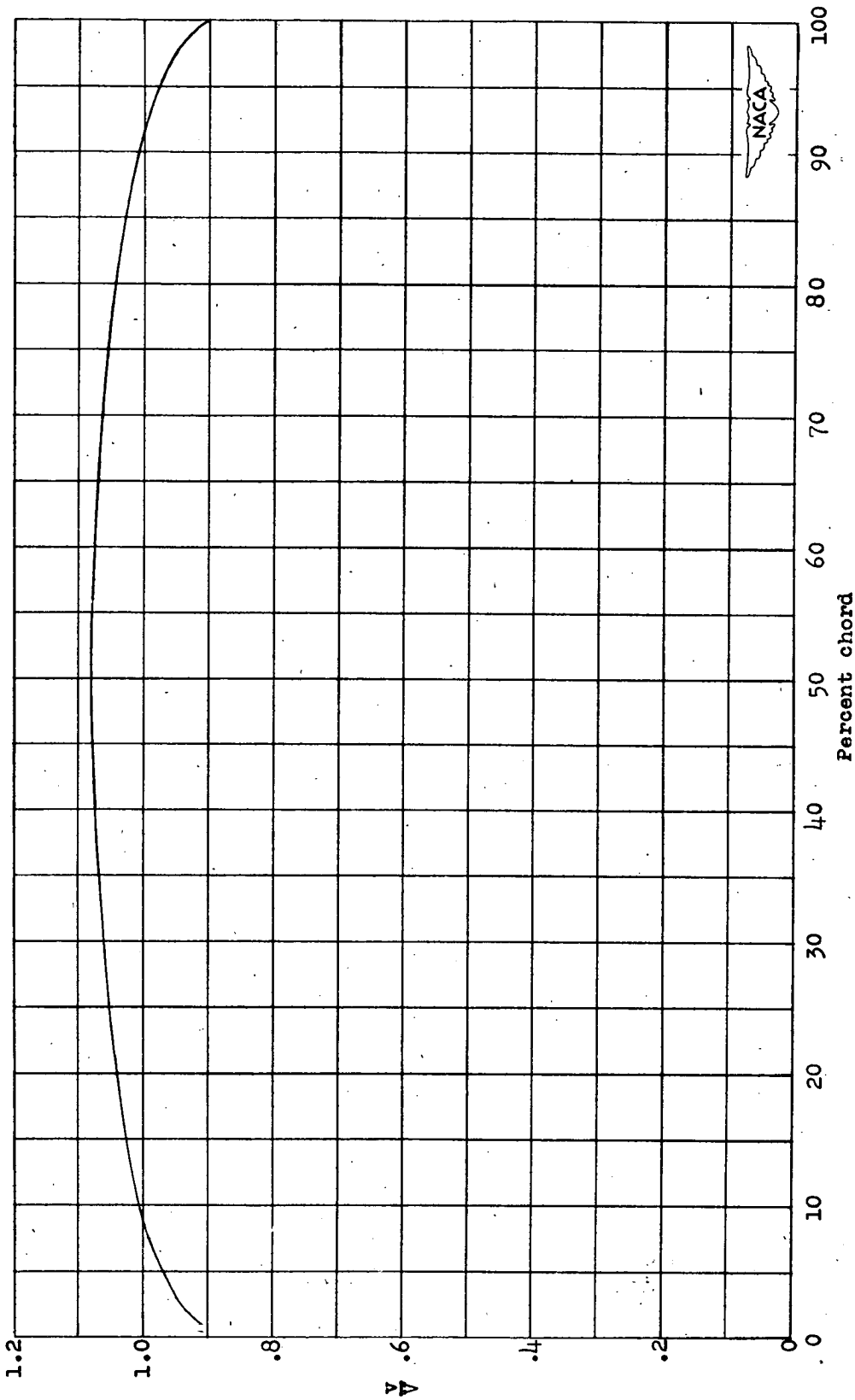

Figure 5.- Velocity distribution for the 6-percent-thick symmetrical circular-arc airfoil section, (reference 1). $\alpha_o = 0°$; $\delta_N = \delta_F = 0°$.

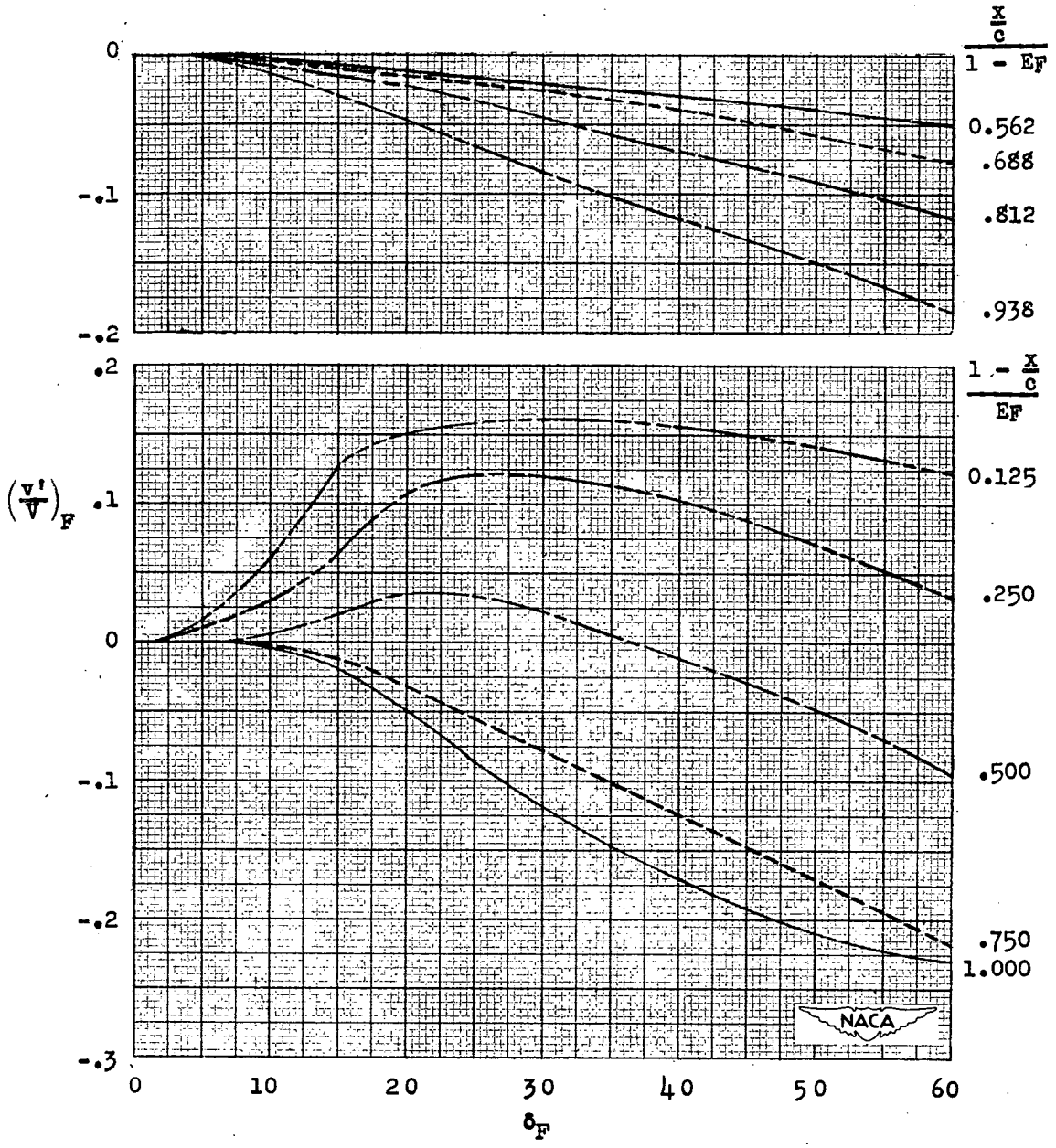

Figure 6.- Variation of $(v'/V)_F$ due to separation in the region of the trailing edge with plain trailing-edge-flap deflection.

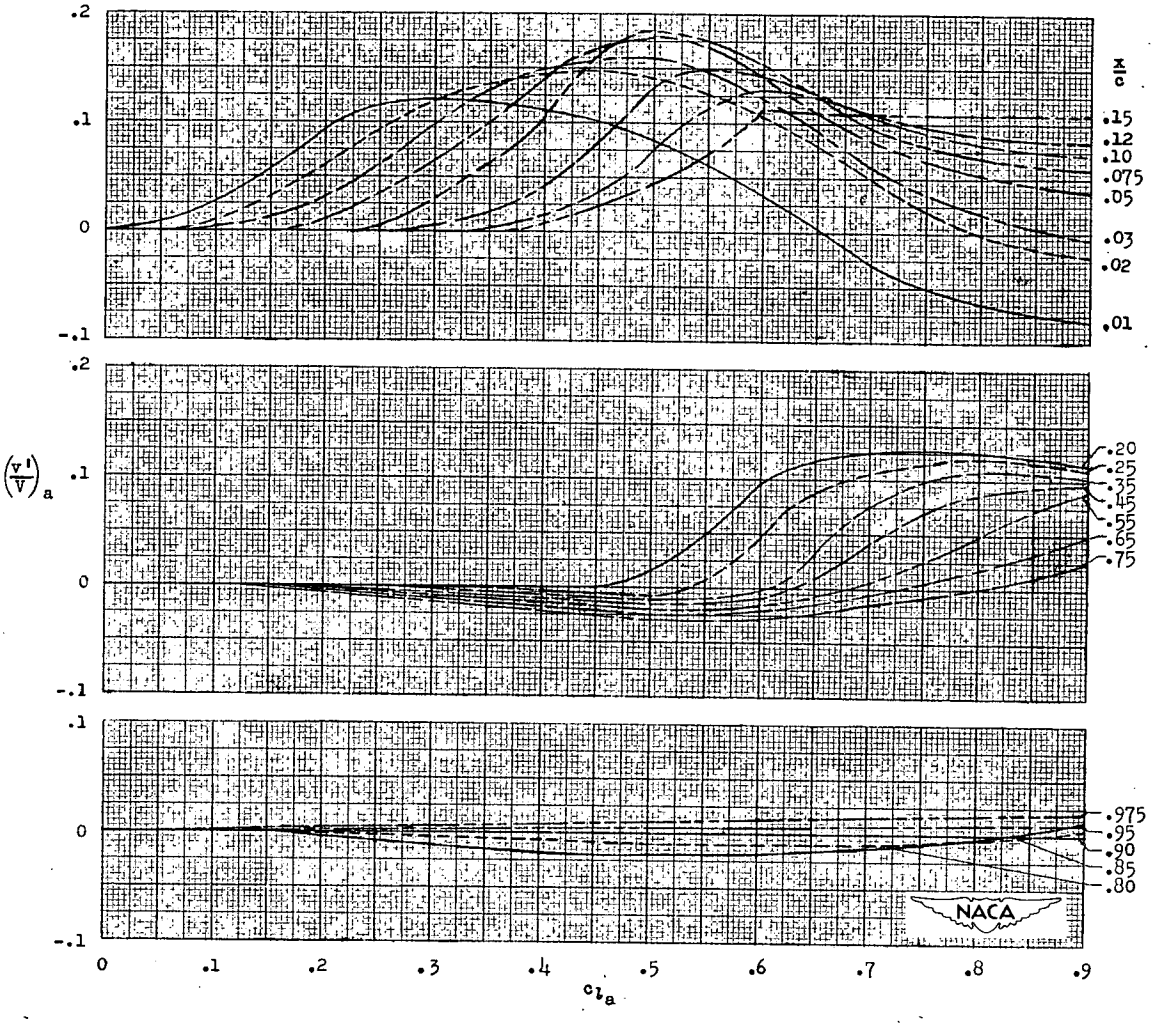

Figure 7.- Variation of $(v'/V)_a$ due to separation near the leading edge with additional lift coefficient.

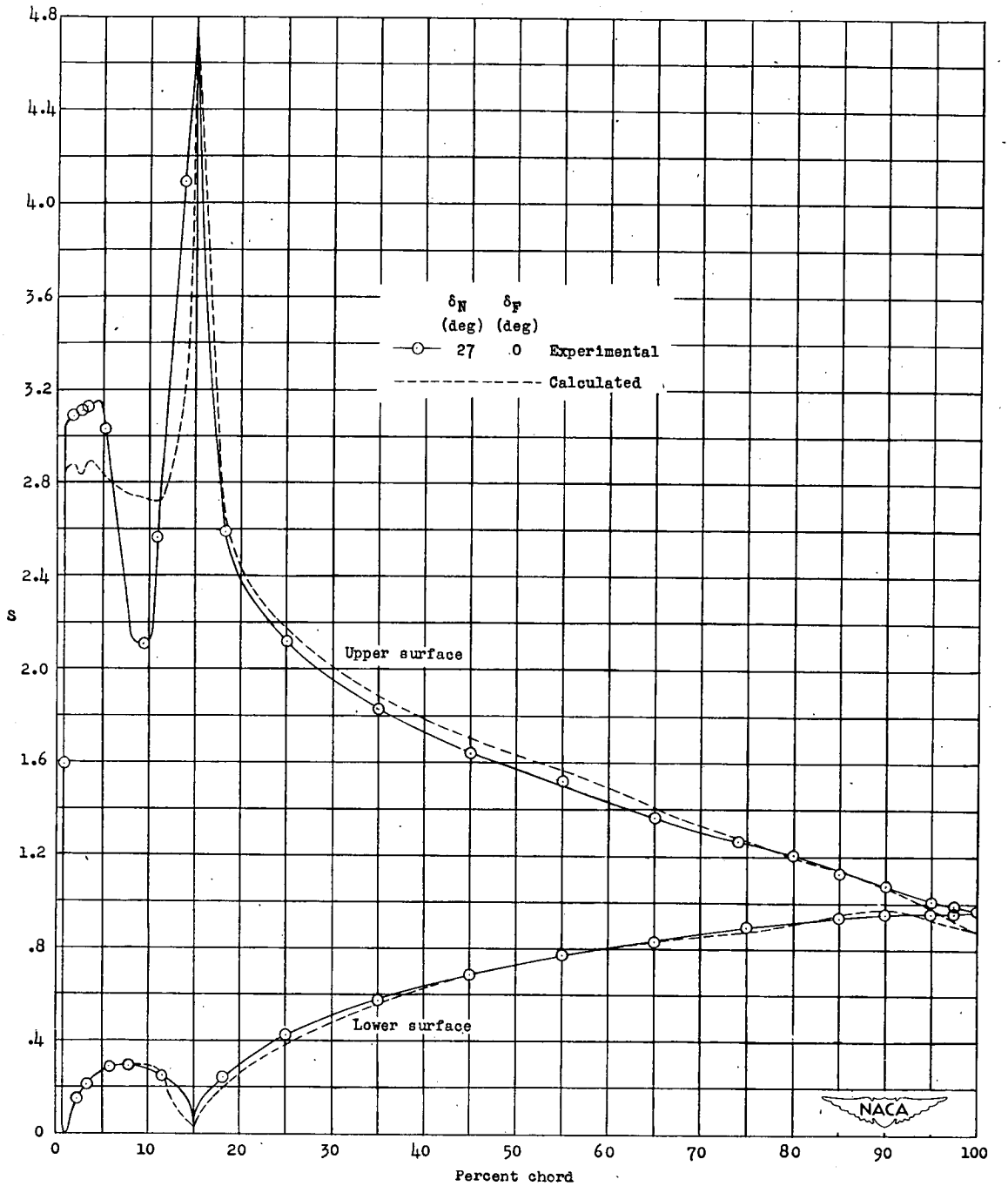

(a) $\alpha_o = 12.2^o$.

Figure 8.- Variation of surface pressure coefficient with percent chord for the 6-percent-thick symmetrical circular-arc airfoil section with 0.15c plain leading-edge flap and 0.20c plain trailing-edge flap.

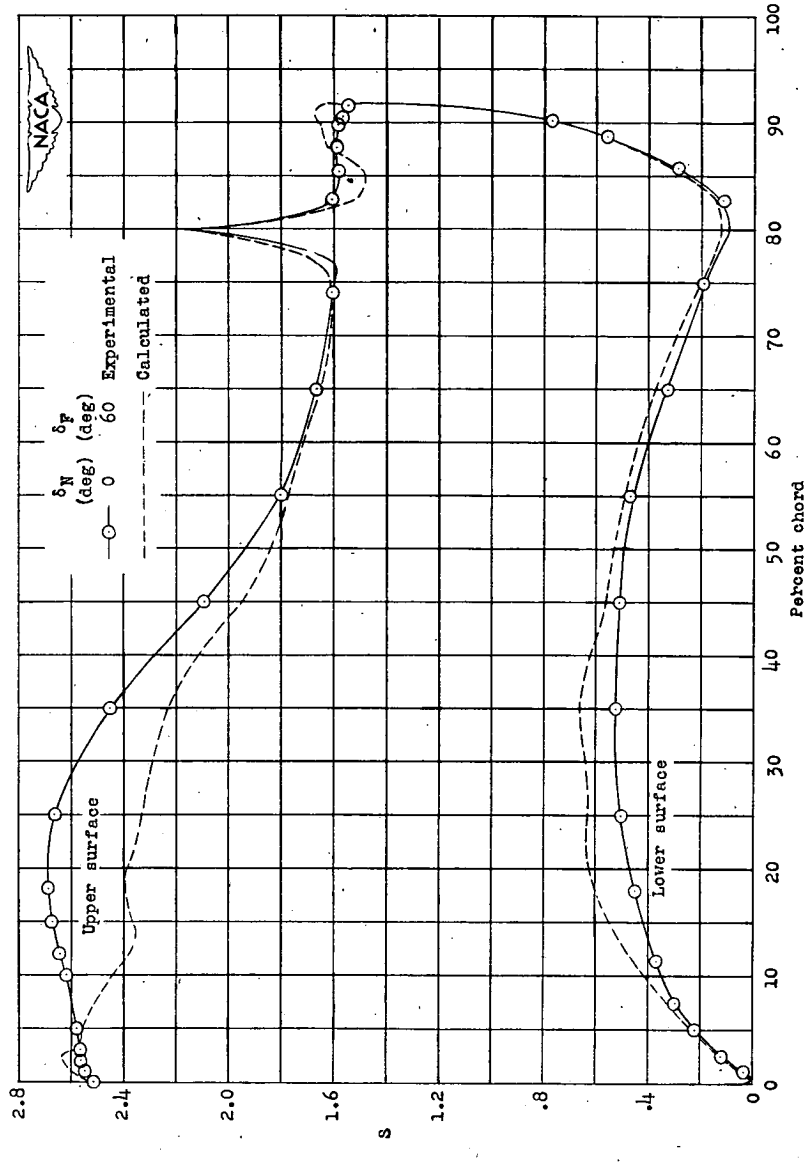

(b) $\alpha_o = 1.0^\circ$.

Figure 8.- Continued.

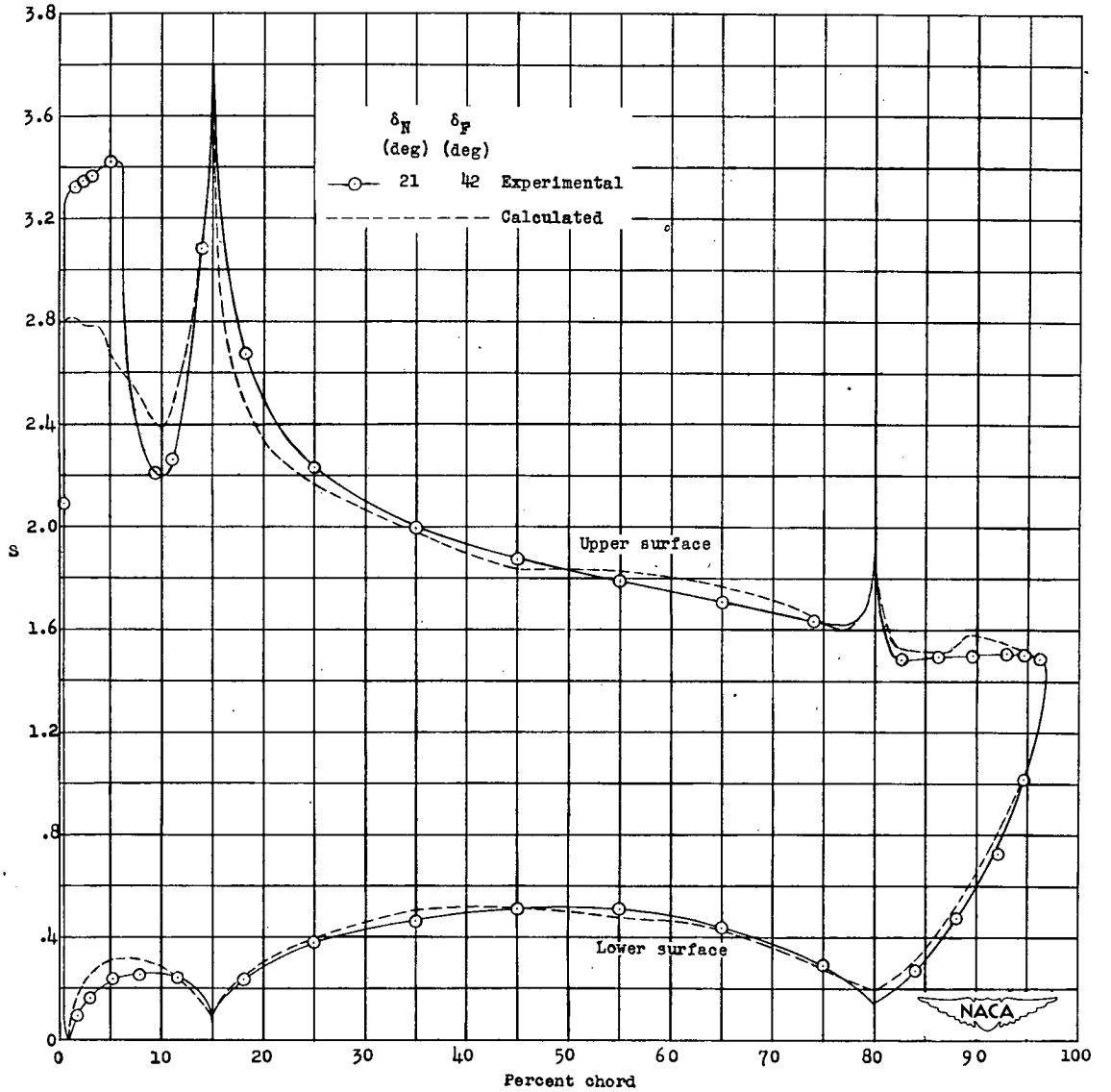

(c) $\alpha_o = 6.1°$.

Figure 8.- Concluded.

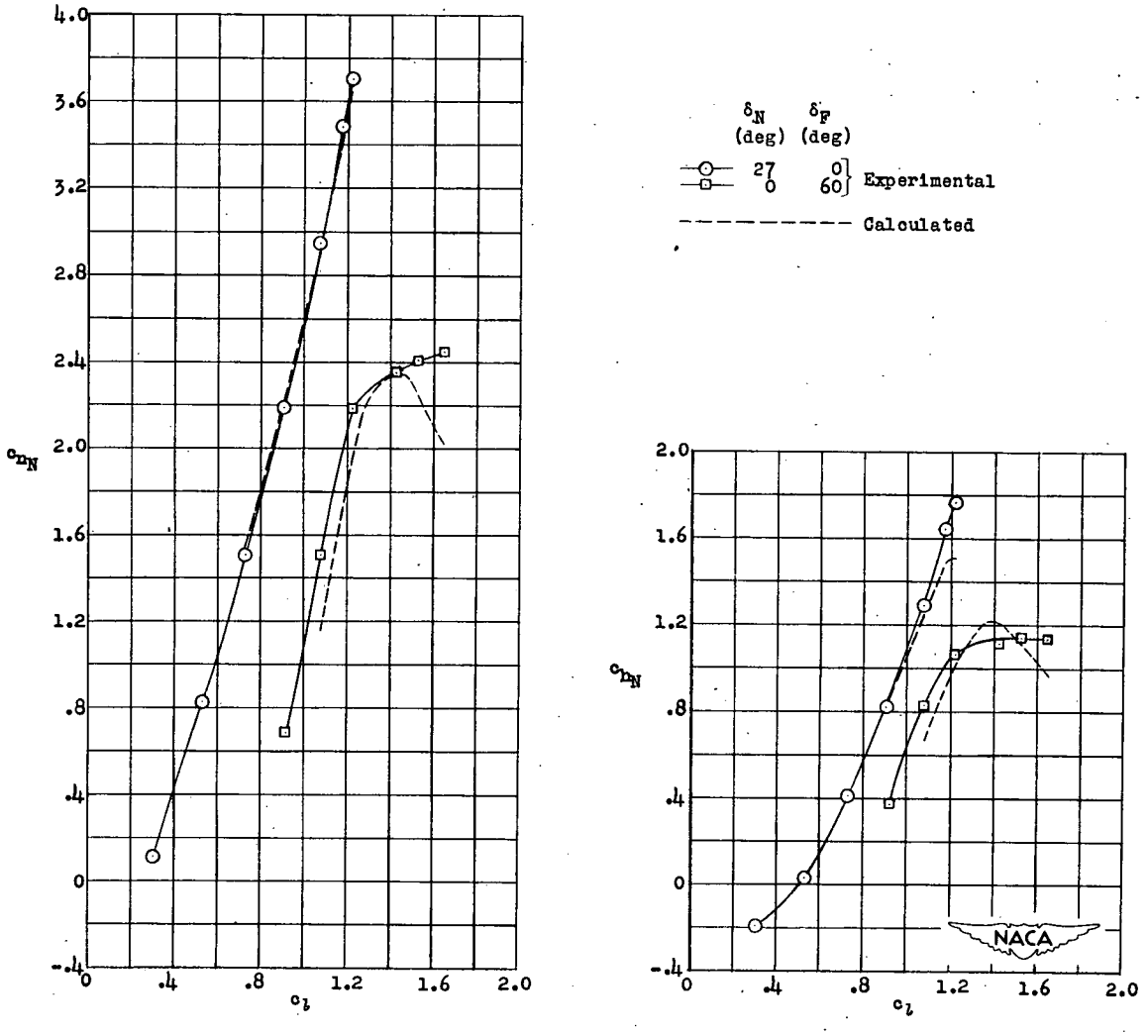

(a) 0.15c plain leading-edge flap.

Figure 9.- Section flap normal-force and hinge-moment characteristics of a 6-percent-thick symmetrical circular-arc airfoil section for individual deflections of the plain leading-edge and trailing-edge flaps.

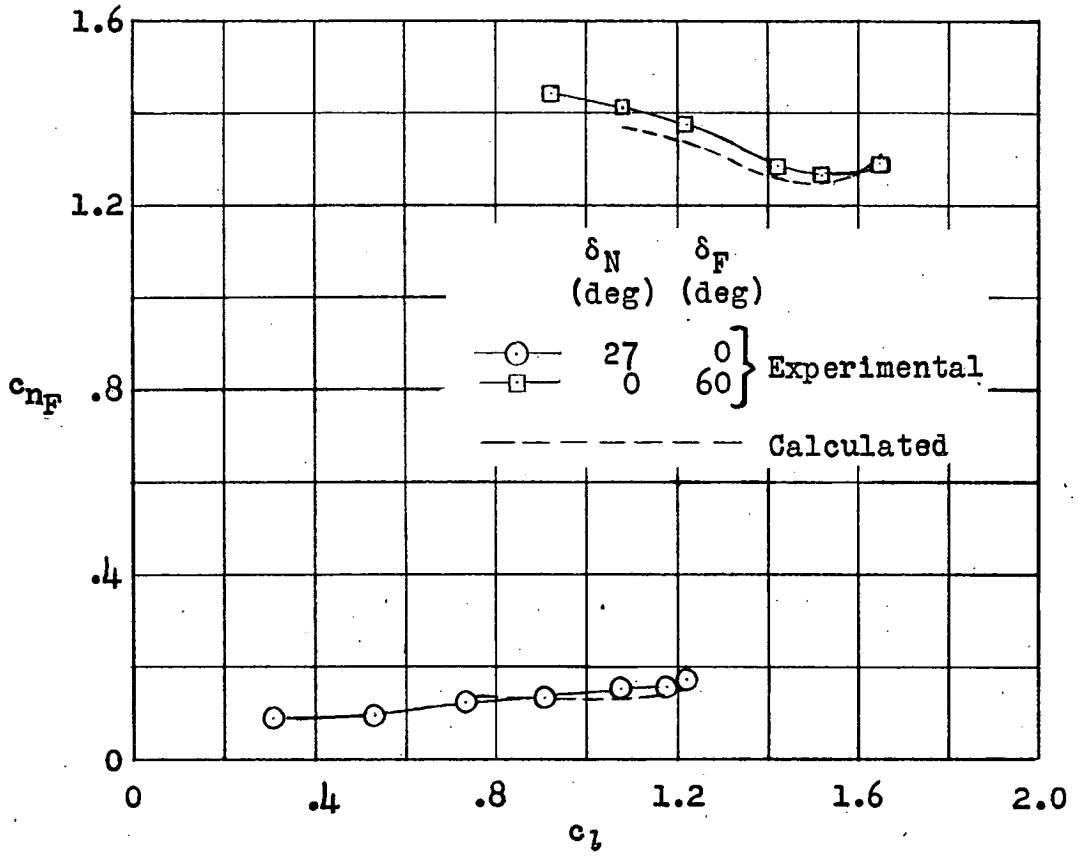

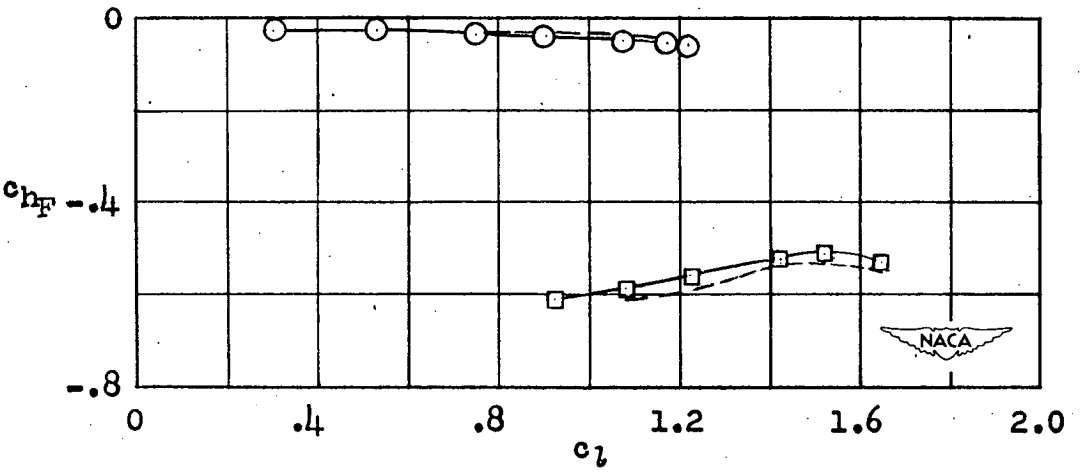

(b) 0.20c plain trailing-edge flap.

Figure 9.- Concluded.

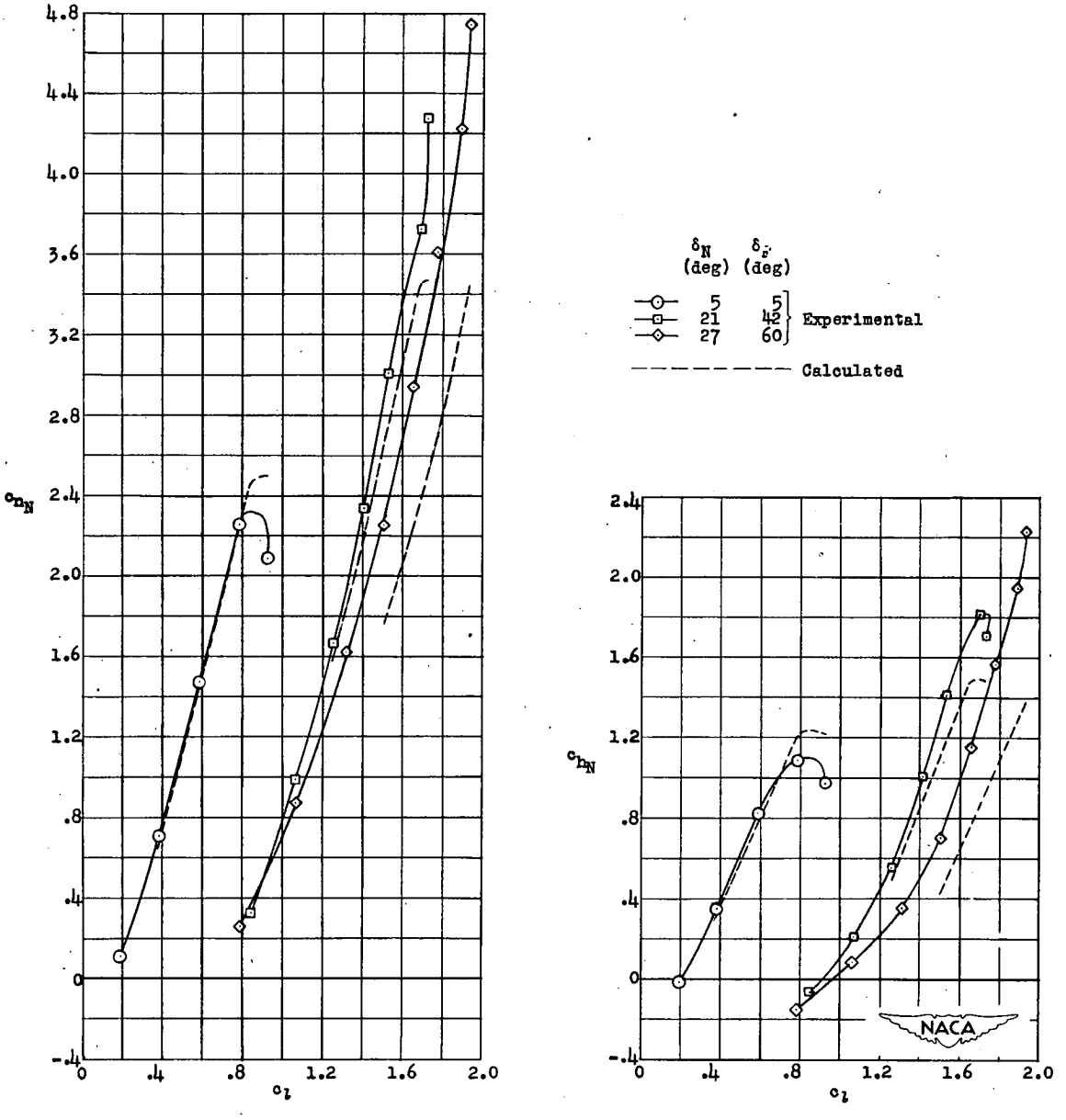

(a) 0.15c plain leading-edge flap.

Figure 10.- Section flap normal-force and hinge-moment characteristics of a 6-percent-thick symmetrical circular-arc airfoil section for combined deflections of the plain leading-edge and trailing-edge flaps.

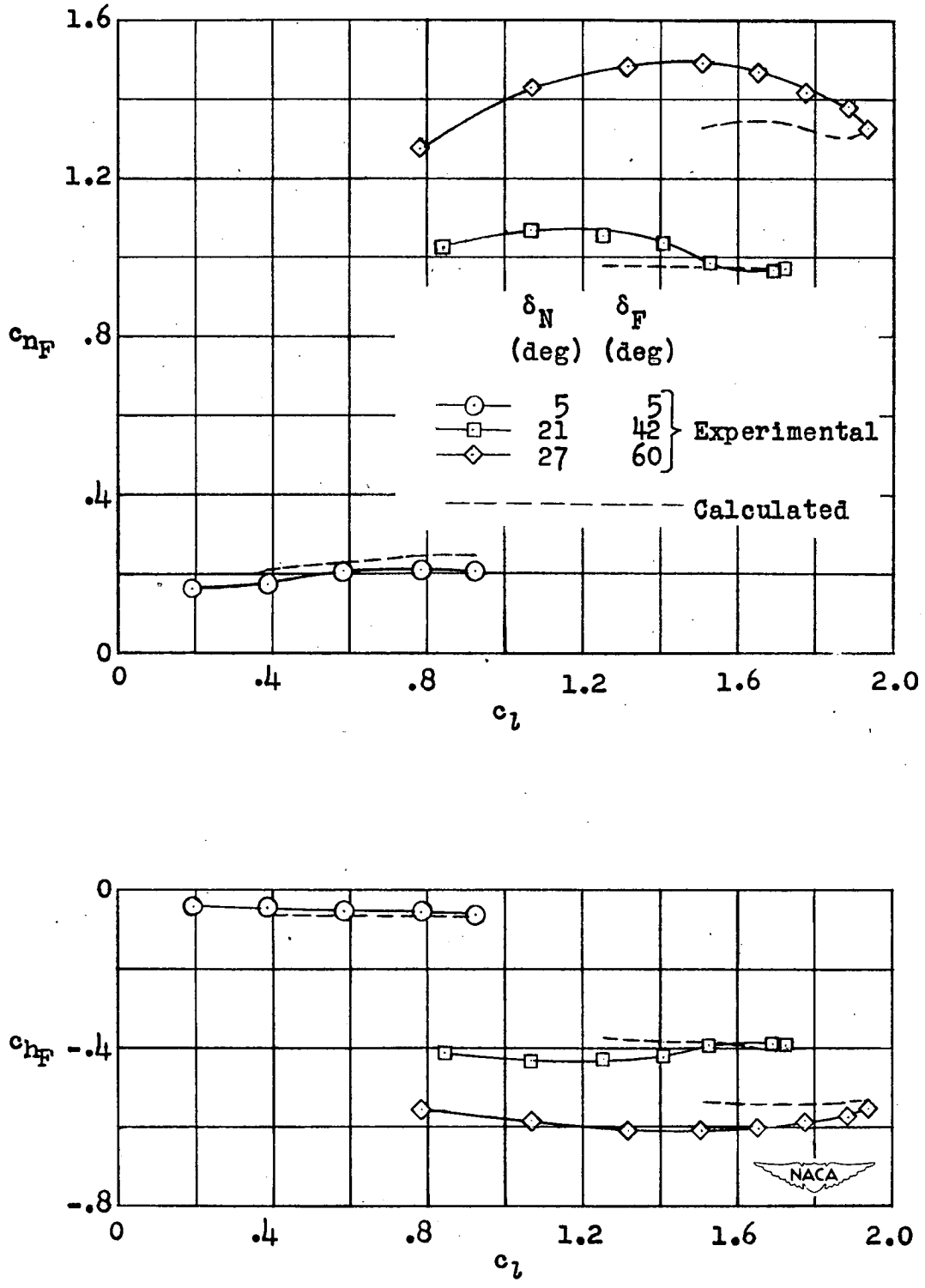

(b) 0.20c plain trailing-edge flap.

Figure 10.- Concluded.